Biochemical signatures of acclimation by Chlamydomonas reinhardtii to different ionic stresses

DOI:
10.1016/j.algal.2018.11.006

Document Version
Accepted author manuscript

Biochemical signatures of acclimation by *Chlamydomonas reinhardtii* to different ionic stresses

Elia D. Charles [a], Howbeer Muhamadali [b,c], Royston Goodacre [b,c], and Jon K. Pittman [a,*]

[a] School of Earth and Environmental Sciences, The University of Manchester, Michael Smith Building, Oxford Road, Manchester M13 9PT, UK

[b] School of Chemistry, Manchester Institute of Biotechnology, The University of Manchester, 131 Princess Street, Manchester M1 7DN, UK

[c] Department of Biochemistry, Institute of Integrative Biology, University of Liverpool, Biosciences Building, Crown Street, Liverpool L69 7ZB, UK

*Corresponding author: Email address: jon.pittman@manchester.ac.uk (J.K. Pittman)

Abstract

Green microalgae can acclimate over short timescales to changing environmental conditions; however, it is unclear how acclimation, or phenotypic adaptation, alters the organism's metabolism and whether there are conserved responses to different stresses. Following six weeks of exposure, *Chlamydomonas reinhardtii* could tolerate 100 mM Na^+, 100 µM Cu^{2+}, and 35 mM PO_4^{3-} and partially tolerate 25 mM NH_4^+, 150 mM Na^+ and 150 µM Cu^{2+}. Acclimation was coincident with increased growth rate and reduced cellular accumulation of reactive oxygen species (ROS), which was indicative of enhanced ROS scavenging. Fourier transform infrared (FT-IR) spectroscopy demonstrated distinct metabolic fingerprints of acclimated cells for each stress condition in comparison to non-acclimated cells and to non-stressed cells. Carbon allocation varied in response to stress but also following acclimation. In particular, Na^+ stress increased intracellular neutral lipid content but this response was significantly reduced in acclimated cells, while carbohydrate content was enhanced in cells acclimated to excess Cu^{2+}. Acclimation of *C. reinhardtii* to Na^+ allowed enhanced tolerance of multiple stresses simultaneously, while the other acclimated cell lines did not display any advantage. While acclimation of *C. reinhardtii* to different ionic stresses elicits distinct metabolic signatures within the cells, enhanced ROS detoxification appears to be a conserved acclimation response.

Keywords: Acclimation, ammonium tolerance, *Chlamydomonas reinhardtii*, copper tolerance, phosphate tolerance, salt tolerance

1. Introduction

Microorganisms can adapt to changing environmental conditions over many generations through heritable genetic alterations, but shorter-term protective responses to environmental perturbations, such as an acute stress, can occur through non-genetic, physiological mechanisms [1]. This shorter-term acclimation process (also referred to as phenotypic adaptations) aims to restore cellular homeostasis, allow survival of the organism and maintain optimal physiological processes [2]. Photosynthetic microorganisms such as green microalgae have evolved mechanisms to acclimate to various environmental perturbations, including high temperature [3], high light [4], salinity [5], metal toxicity [6] and nutrient limitation [7]. These mechanisms can include the synthesis of molecular chaperone proteins, changes to photosynthetic apparatus and photosynthetic efficiency, induction of oxidative stress protective processes, and modifications to metabolic pathways. For example, microalgae may increase synthesis and activity of enzymes to mediate reactive oxygen species (ROS) signalling or enhance ROS scavenging, such as in response to salt stress in *Chlamydomonas reinhardtii* [8, 9]. Photoacclimation to high light in *C. reinhardtii* seems to be mediated by significant metabolic changes including major alteration to nitrogen metabolism [10].

Microalgae will be exposed to many different stresses during their lifetime, and can be exposed to multiple stresses simultaneously. For example, microalgae strains are able to tolerate and grow in toxic wastewater streams, which can contain high concentrations of ammonium (NH_4^+) and phosphate (PO_4^{3-}), salts such as NaCl, and heavy metals, as well as a high bacterial burden and organic pollutants, depending on the source and type of wastewater [11-13]. Microalgae growth in wastewaters has been considered as potentially sustainable means to cultivate biomass for industrial uses such as biofuel feedstock due to the abundance of bioavailable nutrients, while microalgae are also attractive as a low-cost alternative for remediating pollutants from wastewaters [14-16]. Understanding how microalgae can tolerate and grow effectively in such environments is therefore of interest.

Few studies have examined microalgae acclimation to multiple stresses. Furthermore, it is unclear whether there are conserved or distinct responses to different stressors.

A previous analysis of six chlorophyte microalgal strains incubated in a wastewater medium from an urban secondary sewage treatment source found that all strains could quickly (over 6 weeks cultivation) acclimate to the wastewater stress to different degrees, and the acclimation process was associated with an accumulation of photosynthetic pigments and increased activity of the ROS scavenging enzyme ascorbate peroxidase [17]. Another study demonstrated that the microalga *Chlorella sorokiniana* could acclimate to tolerate palm oil mill wastewater, which is rich in organic and inorganic pollutants, causing a change in the metabolic fingerprint of the cells as quantified by FT-IR spectroscopy [18]. However, in both of these cases, it is unclear whether the cells are responding to a specific component of the wastewater or multiple components simultaneously through equivalent or different processes.

This present study therefore aimed to perform a comparative analysis of acclimation by the model microalga *C. reinhardtii* to elevated concentrations of the ionic stressors NH_4^+, PO_4^{3-}, Na^+ and Cu^{2+}, which are consistent with concentrations associated with municipal wastewaters [17]. While many previous studies have examined toxicity, adaptation and acclimation to salinity in microalgae [5, 19], and a few have examined responses to Cu^{2+} toxicity [6, 20], very few prior studies have examined microalgae responses to excess concentrations of NH_4^+ and PO_4^{3-} [21]. The results gathered from this investigation will not only contribute to a broader understanding of microalgae stress response and acclimation to inorganic stressors, but will also inform the applied cultivation of microalgal biomass, such as with regards to optimising wastewater composition for biomass production.

2. Materials and Methods

2.1. Microalgae cultivation and growth measurement

C. reinhardtii (CCAP 11/32C) cells were cultivated under mixotrophic batch conditions in Tris-acetate-phosphate (TAP) medium at 24 °C and 16h:8h light:dark cycle at

150 µmol m^{-2} s^{-1} light intensity on an orbital shaker (120 rpm). TAP media composition was as described previously [22], and included basal concentrations of 0.3 mM Na^+, 6 µM Cu^{2+}, 1 mM PO_4^{3-}, and 7.5 mM NH_4^+. Six versions of modified TAP media containing higher concentrations of these four components was prepared: 100 mM or 150 mM Na-TAP by addition of NaCl; 100 µM or 150 µM Cu-TAP by addition of $CuSO_4$; 35 mM PO_4-TAP by addition of K_2HPO_4; and 25 mM NH_4-TAP by addition of NH_4Cl. In addition, a multi-stressed TAP medium was prepared by addition of NaCl, $CuSO_4$, K_2HPO_4 and NH_4Cl to have a medium containing 100 mM Na^+, 100 µM Cu^{2+}, 35 mM PO_4^{3-} and 25 mM NH_4^+. In all experiments, cell growth was determined by optical density at 750 nm (OD_{750nm}) measurements of cell density using a UV-visible light spectrophotometer (Jenway) and validated by cell counting using a Nexcelom Cellometer T4 (Nexcelom Biosciences), which gave a significant positive correlation between OD_{750nm} values and cell number (Fig. S1). Growth rate (μ) was determined within the exponential growth phase where $\mu = (\ln(N_2) - \ln(N_1)) / (t_2 - t_1)$ where N_1 and N_2 are the cell density values at the early and late exponential phase, respectively, and t_1 and t_2 are the days corresponding to N_1 and N_2, respectively.

2.2. C. reinhardtii acclimation

C. reinhardtii grown in standard TAP medium was acclimated to tolerate individual stresses by weekly re-inoculation into the appropriate stress TAP medium: 100 Na-TAP, 100 Cu-TAP, 35 PO_4-TAP or 25 NH_4-TAP, over a six week period. For each inoculation, cells collected after 7 d batch culture growth were centrifuged at 1500 *g* and concentrated to an OD_{750nm} value of 1.5 then 1 mL of cells was transferred into 39 mL of appropriate TAP medium. At day 7 of each weekly growth period cell density and total chlorophyll concentration was recorded. After the 6 week period, each of the cell cultures were referred to as 'acclimated cells'. Cells acclimated to tolerate 100 mM Na^+ and 100 µM Cu^{2+} conditions were also subsequently acclimated to 150 mM Na^+ and 150 µM Cu^{2+}, respectively. After 3 weeks of acclimation in 100 Na-TAP or 100 Cu-TAP, cells were inoculated into 150 Na-TAP

or 150 Cu-TAP for a further five weeks of re-inoculation, and then referred to as 'acclimated cells'. Each acclimation process was independently replicated three or four times.

2.3. Chlorophyll concentration and chlorophyll fluorescence

A 2 mL volume of late-exponential phase (day 4) cells were collected by centrifugation at 1500 *g* for 5 min. The cell pellets were resuspended and mixed in 2 mL of 96% ethanol until all pigment was extracted from the cells then the cell debris was removed by centrifugation at 1500 *g* for 5 min. Chlorophyll *a* and *b* concentration was measured by absorption spectroscopy and calculated as described by [23]. Total chlorophyll (sum of chlorophyll *a* and *b*) was normalised against cell density value. For non-acclimated and acclimated cells, F_v / F_m ratio, representing the maximum quantum yield of Photosystem II (PSII) was measured using a Heinz Walz PAM-101 chlorophyll fluorimeter and calculated as described [24].

2.4. Fluorescence staining for ROS and neutral lipids

For intracellular ROS measurement, a replicate sample of each acclimated or non-acclimated cell culture was exposed to 100 mM or 150 mM Na^+, 150 µM Cu^{2+}, 35 mM PO_4^{3-}, and 25 mM NH_4^+ for 3 h. Then an equal number of cells at an OD_{750nm} value of 0.5 in a 2 mL sample was harvested by centrifugation at 1500 *g* for 5 min before staining with 85 µM 2',7'-dichlorofluorescein diacetate (DCFH-DA) by incubation for 2 h in the dark at 24 °C then washed twice with phosphate buffer. Fluorescence spectroscopy (Fluoromax) was used to quantify DCFH-DA ROS binding at 485 nm excitation and 530 nm emission wavelengths. Nile red staining was used to quantify neutral lipid content of acclimated and non-acclimated cells after 6 d growth in Na-TAP, Cu-TAP, NH_4-TAP or PO_4-TAP media. Cells were diluted to an OD_{750nm} value of 0.5 then 740 µL of culture was added to 250 µL DMSO and 10 µL Nile red stain (50 mg mL^{-1}). Cells were then incubated at 40 °C for 10 min in the dark. Fluorescence spectroscopy (Fluoromax) was then used to determine Nile red lipid binding at 530 nm emission and 575 nm excitation wavelengths.

146

147 *2.5. Fourier transform-infrared (FT-IR) spectroscopy*

148 Cell cultures were normalized to an OD_{750nm} value of 0.7 and 10 mL was centrifuged
149 at 1800 *g* for 5 min then the supernatant was removed and the cells washed twice in 1.5 mL
150 of sterile 0.9% (v/v) NaCl solution, before resuspension of each cell pellet in 1 mL of 0.9%
151 (v/v) NaCl to equivalent to an OD_{750nm} value of 7.0. For each replicate sample, 2 x 20 µL cell
152 suspension was added onto a 96-well silicon microplate, with each sample being oven dried
153 at 50 °C for 1 h before the second volume was added. An Equinox 55 FT-IR spectrometer
154 (Bruker Corporation), equipped with a deuterated triglycerine sulfate detector with a HTS-XT
155 high-throughput microplate extension was used to collect the FT-IR spectra from the plate.
156 Spectra were collected over the wavenumber range 4000 – 600 cm^{-1}, following previously
157 reported settings [25]. Spectra were pre-processed using extended multiplicative signal
158 correction (EMSC2) [26]. All preprocessed data were subjected to principal components
159 analysis (PCA) followed by discriminant function analysis (PC-DFA) using MATLAB. PCA
160 was used to reduce the dimensionality of the data, and DFA was applied to maximize
161 between-group variance while minimizing within-group variance [27]. Band assignments
162 were determined as described previously [28].

163

164 **3. Results**

165 *3.1. Acclimation of C. reinhardtii to individual stressors*

166 *C. reinhardtii* cultures were treated with concentrations of Na^+, Cu^{2+}, PO_4^{3-} and NH_4^+
167 that elicited a stress response in comparison to the conditions of cultivation in standard TAP
168 medium. 100 mM Na^+ (compared to 0.3 mM Na^+), 100 µM Cu^{2+} (compared to 6 µM Cu^{2+}), 35
169 mM PO_4^{3-} (compared to 1 mM PO_4^{3-}), and 25 mM NH_4^+ (compared to 7.5 mM NH_4^+) each
170 caused significantly reduced cell density (Fig. S1 and Fig. S2) and reduced growth rate,
171 although the growth rate inhibition for the 100 µM Cu^{2+} treatment was less than for the other
172 stresses (Fig. 1). Cells were exposed to each stress during sequential 7 d batch cultures
173 over a 6-week period with cell density measured at the end of each week. Over the period of

174 acclimation, in response to 100 mM Na^+, 100 µM Cu^{2+} and 35 mM PO_4^{3-} cell density of *C.*
175 *reinhardtii* increased mostly uniformly week by week to a level equivalent to that of the non-
176 stressed control by the sixth week (Fig. 1A) and growth rate was significantly increased for
177 the cultures acclimated to Na^+ and PO_4^{3-} (Fig. 1C). The process of acclimation to 25 mM
178 NH_4^+ was different to the other three stress treatments. Following the first week of batch
179 culture, there was a substantial NH_4^+ toxicity demonstrated by significant reduction in cell
180 density over the next three weeks of batch cultures, however, in the final two weeks, cell
181 density increased significantly but did not increase above 75% of the non-stressed control
182 (Fig. 1A). Nevertheless, the NH_4^+ acclimated cells by the final week of treatment did display
183 significantly higher growth rate in comparison to non-acclimated cells (Fig. 1C). The profiles
184 of weekly total chlorophyll concentration during the periods of acclimation for each treatment
185 were equivalent to the cell density profiles (Fig. S3A).

186 The 100 mM Na^+ and 100 µM Cu^{2+} cells were sub-cultured into 150 mM Na-TAP and
187 150 µM Cu-TAP media, respectively, to determine whether the cells could acclimate to a
188 higher concentration of Na^+ or Cu^{2+}. While serial inoculation in 150 mM Na^+ media increased
189 cell density over time and significantly increased growth rate (Fig. 1), tolerance to this higher
190 concentration of Na^+ could not reach the level of the 100 mM Na^+ acclimated cells or the
191 non-stressed control. *C. reinhardtii* was able to grow in 150 µM Cu^{2+}, however, there was no
192 significant improvement over time (Fig. 1B) and growth rate was even significantly lower in
193 the 150 µM Cu^{2+} acclimated cells compared to non-acclimated cells (Fig. 1C).

194 Acclimated and non-acclimated cells were also examined for photosynthetic
195 parameters. While total chlorophyll concentration was either unchanged or moderately
196 increased in the cells acclimated to 100 mM Na^+, 100 µM Cu^{2+} or 35 mM PO_4^{3-}, it was
197 significantly reduced in the 25 mM NH_4^+ exposed cells (Fig. S3). However, the F_v / F_m ratio,
198 which represents the maximum quantum yield of PSII and is routinely used as an indicator of
199 stress [24], was unchanged between non-acclimated and acclimated cells in response to
200 NH_4^+ treatment (Fig. S3C). Likewise, there was no significant change in F_v / F_m ratio in

response to Cu^{2+} or PO_4^{3-} exposure, while both concentrations of Na^+ significantly reduced F_v / F_m ratio value and acclimation to Na^+ significantly increased F_v / F_m ratio.

3.2. Oxidative stress response

Intracellular ROS accumulation was measured in acclimated and non-acclimated cells following exposure to excess Na^+, Cu^{2+}, PO_4^{3-} and NH_4^+. ROS are a common by-product of metabolic processes within all cells [29] therefore non-stressed cells were also stained with DCFH-DA to determine background levels of ROS to quantify ROS induction relative to non-stressed control cells. All treatments significantly increased intracellular ROS after 3 h in non-acclimated cells, with NH_4^+ exposure inducing the highest increase in comparison to controls (Fig. 2). In acclimated cells there was a comparative significant reduction in ROS accumulation for all treatments. Cells acclimated to 150 mM Na^+ and 150 µM Cu^{2+} induced ROS to approximately 30% increase relative to the control compared to an approximately 70-80% increase for the non-acclimated cells. Furthermore, for cells acclimated to 100 mM Na^+, 35 mM PO_4^{3-} and 25 mM NH_4^+ there was no significant increase in ROS compared to the non-stressed control cells (Fig. 2).

3.3. Metabolic fingerprints of acclimation by FT-IR spectroscopy

FT-IR spectroscopy allowed assessment of the metabolic response of *C. reinhardtii* to the ionic stresses, and an evaluation of the metabolic signatures of acclimation. Replicate FT-IR spectra were collected from non-acclimated cells cultivated in each stress condition (Fig. S4). These spectra were statistically analysed using supervised multivariate analysis PC-DFA to identify changes in metabolic fingerprints of the cells after 6 d growth (Fig. S5). There were clear differences between control non-stressed cells and all stressed cells on the basis of clustering within the PC-DFA scores plot. There was some overlap between the Na^+, Cu^{2+} and PO_4^{3-} exposed cells while the NH_4^+ treated cells clustered apart from all others on the basis of discriminant function 1 (DF1) and 2 (DF2) (Fig. S5A). DF loading plots indicated that the stressed non-acclimated cells were distinguished by changes in

polysaccharides (1200-900 cm^{-1}) with 25 mM NH_4^+ stressed cells having the lowest polysaccharide content (Fig. S5B). Additionally, both DF1 and DF2 loadings highlight substantial variation between spectra, such that the NH_4^+ stressed cells had higher absorbance in amide I and II regions. The Na^+ stressed cells could be further distinguished from the Cu^{2+} and PO_4^{3-} exposed cells on the basis of DF3, which was associated with changes to lipid and carbohydrate content (data not shown).

With the demonstration that FT-IR spectroscopy can be used to distinguish between each of the stress treatments, comparisons were made between the acclimated and non-acclimated cells. PC-DFA was able to generate two distinct clusters which separate Na^+ acclimated cells from non-acclimated cells, especially for the 100 mM Na^+ acclimated cells, which partially overlapped with the non-stressed control cells (Fig. 3A). The loading plot indicates that many spectral features were changed between the acclimated and non-acclimated cells on the basis of DF1 and DF2 (Fig. 3C). The changes in spectra characteristics for the 100 mM Na^+ acclimated cells were particularly attributable to increase in fatty acid associated peaks (2957-2852 cm^{-1}), increase in amide I and II (~1655 and ~1545 cm^{-1}), and substantial variation with respect to the polysaccharide region. PC-DFA likewise generated distinct clusters between non-acclimated cells grown in 100 µM and 150 µM Cu^{2+} and the acclimated cells, which were in turn clearly distinct from the spectra of control, non-stressed cells (Fig. 3B). DF2 explains most of the changes due to acclimation to Cu^{2+} in comparison to non-acclimated, Cu^{2+}-stressed cells, while DF1 explains the variation between control and acclimated cells. DF1 loadings highlight significant variation between spectra at wavenumber 1745 cm^{-1}, typically attributed to ester functional groups from lipids and fatty acids (Fig. 3D). Cu^{2+} acclimated cells were highly distinct from the control samples and non-acclimated cells on the basis of amide I and amide II signatures. Additionally, spectra indicate that acclimated cells had higher absorbance within carbohydrate peaks in comparison to control and non-acclimated cells.

The analysis of the spectra from PO_4^{3-} and NH_4^+ treated experiments showed substantial variation and tight clustering between non-stressed control, non-acclimated

stressed, and acclimated cell populations (Fig. 4A and B). Changes in spectra due to PO_4^{3-} acclimation were explained predominantly by DF1. Thus, according to DF1 loadings, acclimation to PO_4^{3-} induced positive changes in amide I and reduction in carbohydrate (Fig. 4C). For the NH_4^+ treatment, acclimated cells were particularly clustered on the basis of DF2 (Fig. 4B), with DF2 loadings indicating variation with respect to amide I, a change within the ν_{as}P=O bonds of nucleic acids, phosphoryl groups, or phosphorylated proteins (~1245 cm^{-1}), and further variation within the polysaccharide peaks (Fig. 4D).

The overall comparison of the PC-DFA clustering patterns suggests that the cells are benefiting from acclimation to Na^+, PO_4^{3-}, and NH_4^+, as the acclimated cells are clustering on the same side (according to DF1) of the control samples on the PC-DFA scores plots. Whilst the Cu^{2+} acclimated cells are clustering on the opposite side of the control samples which suggest that these cells are not benefiting as much from this process, which is in complete agreement with our findings based on the comparison of changes in growth rate (Fig. 1C) and profiles (Fig. S2) of the cells under these conditions.

3.4. Changes in carbon allocation: lipids and carbohydrates

Non-acclimated and acclimated cells were analysed individually to assess the effect acclimation had on cellular carbon allocation. It has been previously demonstrated that FT-IR spectroscopy can reliably and accurately quantify lipid and carbohydrate composition of algal cells and that data from individual spectra peaks can be validated by conventional methods [30-32]. Using FT-IR data the lipid:amide I and carbohydrate:amide I ratios were used for relative quantitation and to identify significant changes in total lipids and carbohydrates in response to the acclimation treatments. Several investigations have previously used both amide I and amide II peaks to quantify relative amounts of metabolites including lipids and carbohydrates [32-34]. In general lipid:amide I ratio values indicated no significant variation between acclimated and non-acclimated cells on the basis of total lipid (data not shown). To examine this further with respect to neutral storage lipids, including triacylglycerol, cells were stained with Nile red to measure neutral lipid accumulation after 6

d growth. Storage lipid accumulation is a common stress response in green microalgae such as *C. reinhardtii*, and all stresses apart from 25 mM NH_4^+ induced a significant increase in neutral lipid accumulation (Fig. 5A). Acclimation to both 100 mM and 150 mM Na^+ significantly reduced neutral lipid content of cells in comparison to non-acclimated cells, whereas Cu^{2+} and PO_4^{3-} acclimation had no effect.

Changes in total carbohydrate content as determined by carbohydrate:amide I ratio were observed in many of the treatments. 25 mM PO_4^{3-} and 100 mM Na^+ significantly increased carbohydrate content in comparison to non-stressed control while acclimation to these two conditions significantly reduced carbohydrate content (Fig. 5B). In contrast, there was a substantial significant increase in carbohydrate content in both sets of Cu^{2+} acclimated cells while non-acclimated cells exposed to either Cu^{2+} concentration were equivalent to non-stressed control.

3.5. Tolerance of acclimated cells to multiple simultaneous stresses

All acclimated cells were grown in medium containing elevated concentrations of Na^+ (100 mM), Cu^{2+} (100 µM), PO_4^{3-} (35 mM) and NH_4^+ (25 mM) together, in order to assess whether acclimation to any of the individual stresses had increased the tolerance of *C. reinhardtii* to a multi-stressed environment. The multiple stress treatment was very toxic to non-acclimated cells and resulted in a substantial decrease in cell density and total chlorophyll concentration by nearly 60% in comparison to non-stressed control cells (Fig. 6). Most of the acclimated cell types showed no additional tolerance on the basis of no significant difference in total chlorophyll concentration or cell density. Only the Na^+ acclimated demonstrated a degree of multi-stress tolerance; the 100 mM Na^+ acclimated cells displayed a significantly higher cell density compared to the non-acclimated cells, and the 150 mM Na^+ acclimated cells had significantly higher chlorophyll content (Fig. 6). This distinction was also apparent on the basis of FT-IR spectra analysis, with strong clustering observed between the 100 mM Na^+ acclimated cells separate from the non-stressed control cells and from the cluster containing the non-acclimated multi-stressed cells and the Cu^{2+},

313 NH_4^+ and PO_4^{3-} acclimated cells (Fig. 7A). Mostly DF2 explains the variation between the
314 Na^+ acclimated, multi-stress tolerant cells and the multi-stress sensitive cells, particularly
315 associated with spectral changes in the amide I and amide II regions (Fig. 7B).
316
317 **4. Discussion**
318 Acclimation responses in photosynthetic microorganisms such as *C. reinhardtii* have
319 been previously studied for stresses including high light, high or low temperature, and
320 salinity, highlighting the importance of specific transcriptional, proteomic or metabolic
321 changes in controlling the acclimation to these different stresses [3-5, 10, 35]. While there
322 are clear distinctions between these particular acclimation responses, previous studies have
323 not performed side-by-side comparisons of acclimation to different stresses under identical
324 conditions with the same microalgae strain in order to determine whether there are
325 conserved responses or highly distinct responses. This study therefore examined four
326 different but related ionic stresses: elevated concentrations of Na^+, Cu^{2+}, PO_4^{3-} and NH_4^+.
327 Well characterised green microalgae stress indicators (growth rate, chlorophyll
328 concentration, F_v / F_m ratio, storage lipid accumulation and ROS accumulation) demonstrated
329 that the concentrations of the ions chosen elicited stress in non-acclimated cells and that
330 acclimation by *C. reinhardtii* allowed strains to fully tolerate (for 100 mM Na^+, 100 µM Cu^{2+}
331 and 35 mM PO_4^{3-}) or partially tolerate (for 150 mM Na^+, 150 µM Cu^{2+} and 25 mM NH_4^+) the
332 individual stressors. Apart from for the Na^+ stresses, the F_v / F_m ratio, which is the ratio of
333 variable to maximum chlorophyll fluorescence and an indicator of the efficiency of PSII, was
334 a poor indicator of stress (Fig. S3C). This was particularly surprising for the NH_4^+ treatment
335 since this stress caused a significant drop in chlorophyll concentration (Fig. S3A).
336 Furthermore, high NH_4^+ stress inhibits photosynthesis in many species of algae by directly
337 competing with water as an electron donor to PSII thereby significantly reducing
338 photosynthetic efficiency [36]. Likewise, Cu^{2+} exposure has been previously shown to inhibit
339 photosynthetic activity [37, 38]. It has previously been argued that chlorophyll fluorescence

responses, and in particular the F_v / F_m ratio poorly correlates to microalgae biomass, growth rate and nutrient status, and may therefore be a poor indicator of physiological status [39].

All stressors induced intracellular production of ROS in non-acclimated cells within 3 h of exposure as determined through use of the DCFH-DA reporter, and a clear conserved response between all acclimated strains was a substantial decrease in ROS production, although the relative levels of ROS reduction varied (Fig. 2). Taken together, this suggests that acclimated cells may have had enhanced antioxidant capabilities. This is consistent with previously observed mechanisms of acclimation by microalgae to multiple stresses. Species such as *Chlorella luteoviridis* were shown to acclimate to wastewater conditions associated with reduced ROS accumulation and increased activity of ascorbate peroxidase [17]. ROS accumulation by the individual stresses as observed here was expected as most of these stresses, including salinity, Cu^{2+}, and NH_4^+ were known to lead to the production of internal ROS [8, 40, 41]. Cu^{2+} can directly induce ROS by participating in Fenton chemistry [40], while NH_4^+ has been shown in higher plants to induce redox imbalances through reactions with the mitochondrial electron transport chain [41] as well as by induction of the urea cycle, which increases production of nitric oxide [42]. Increased antioxidant activities in microalgae as a tolerance mechanism to salt stress and Cu^{2+} toxicity have previously been observed [8, 43-45] and is likely to be a component of the acclimated *C. reinhardtii* cells. In contrast, the significant ROS reduction in the NH_4^+ acclimated cells may be partly due to a reduction in NH_4^+ uptake rather than antioxidant mechanisms, since nitric oxide production inhibits the NH_4^+ uptake pathway therefore blocking further ROS induction [42].

No previous studies have examined links between PO_4^{3-} toxicity and acclimation to redox status and antioxidant mechanisms. Indeed, current literature regarding PO_4^{3-} toxicity is very limited for both plants and algae. However, eutrophication is an increasing problem for some freshwaters and agricultural land leading to PO_4^{3-} toxicity symptoms [46, 47]. Microorganisms including microalgae can store excess PO_4^{3-} as internal poly-PO_4^{3-} [48] and are therefore able to partly buffer and maintain internal PO_4^{3-} concentrations. A recent study examined the response to a “large excess” of PO_4^{3-} up to 250 mg L^{-1} in *Chlorella regularis*

and found inhibited cell growth and reduced cell viability linked to impaired cellular structure and high concentrations of intracellular poly-PO_4^{3-} [49]. This study has exposed *C. reinhardtii* to 35 mM PO_4^{3-} (equivalent to >3 g L^{-1}) although it should be noted that the strain had been previously continuously cultivated in TAP medium with an already high PO_4^{3-} concentration of 1 mM (equivalent to 95 mg L^{-1}) and this *C. reinhardtii* strain may therefore have already partially acclimated (or adapted) to relatively high PO_4^{3-} before incubation in 35 mM PO_4^{3-}.

C. reinhardtii acclimated strongly to the lower concentrations of Na^+ and Cu^{2+} but only partly to 150 mM Na^+ and 150 µM Cu^{2+}. High Na^+ concentrations will inhibit cell growth by causing osmotic stress and impaired Na^+/K^+ homeostasis, in particular resulting in competitive inhibition of K^+ dependent enzymes [50]. Therefore Na^+ acclimation mechanisms will require enhanced osmoregulation and intracellular Na^+ regulation, such as through Na^+ sequestration [35, 51]. Cu^{2+} is known to be a potent inhibitor of microalgal growth by a variety of different mechanisms, which include its ability to displace essential metal ions in enzymes, interact with thiol groups of proteins, induce oxidative stress and disrupt photosynthetic activity, leading to significantly reduced growth rate and cell viability [20, 52]. A previous attempt to acclimate a *Chlorella* sp. to tolerate higher concentrations of Cu^{2+} was unsuccessful [6], so species-specific differences may explain the ability of *C. reinhardtii* to successfully acclimate to high Cu^{2+}. There are various mechanisms by which a cell could gain tolerance to Cu^{2+} including ligand binding and internal sequestration [53]. Future experiments will be needed to identify the exact mechanisms involved within the Na^+ and Cu^{2+} acclimated *C. reinhardtii*.

The acclimation of *C. reinhardtii* to 25 mM NH_4^+ was challenged by a severe reduction in cell density following the first three repeats of re-inoculation into NH_4-TAP medium during Weeks 2 to 4 of the acclimation process (Fig. 1A). This is in agreement with previous studies which have identified a mean inhibitory concentration of ~24 mM NH_4^+ and a mean toxic concentration of ~39 mM NH_4^+ for Chlorophyceae algae [21]. As discussed above, NH_4^+ stress is known to severely inhibit photosynthesis, which would hamper improvements to growth. However, in all experiments *C. reinhardtii* cultivation was

396 mixotrophic, by using a combination of photosynthesis as well as using organic carbon in the
397 form of acetate. The ability of the NH_4^+ stressed cells to utilise acetate even if autotropic
398 growth was compromised, coupled with an NH_4^+-induced increase in photorespiration [42],
399 may explain the ability of the cells to withstand the NH_4^+ toxicity and subsequently start to
400 show enhanced tolerance by Week 5 and 6. Future investigations should therefore compare
401 acclimation without acetate to confirm whether the NH_4^+ acclimation process was partly due
402 to a change in energy metabolism, or monitor the acetate levels in the medium to quantify its
403 assimilation. Furthermore, acclimation to each of the ionic stresses should be examined in
404 future under autotrophic conditions in contrast to the mixotrophic conditions of this present
405 study.

406 Both the initial stress responses in non-acclimated cells and the response to
407 acclimation could be clearly detected and distinguished on the basis of FT-IR spectra
408 coupled with multivariate analysis. While each stress treatment sample could be
409 differentiated from each other and from the non-stressed samples according to the PC-DFA
410 scores plots, there was some overlap between the Cu^{2+}, Na^+ and PO_4^{3-} treatments indicating
411 related metabolic responses, while NH_4^+ stress yielded a very distinct metabolic fingerprint
412 compared to all other treatments and the control (Fig. S5A). This is in line with the
413 substantial toxicity caused by 25 mM NH_4^+ as discussed above. Substantial metabolic
414 variation between the NH_4^+ treated cells and the other treatments was due to internal carbon
415 storage. During times of stress microalgae redirect more energy in the form of ATP and
416 NADPH to carbon storage in the form of lipid or carbohydrates rather than algal biomass for
417 growth [54]. Extensive microalgae research has studied this during nitrogen and phosphorus
418 deficiency [32]. In response to such stresses, microalgae synthesise a diverse range of
419 lipids, mainly neutral storage lipids such as triacylglycerols and to a lesser extent membrane
420 lipids [55]. The Na^+, Cu^{2+} and PO_4^{3-} stress treatments induced significant accumulation of
421 either storage lipid and/or carbohydrate, while the NH_4^+ treatment showed no lipid increase
422 relative to control and a significant reduction in carbohydrate (Fig. 5), which is likely to be
423 due to change in starch abundance [32]. The substantial lipid induction observed in

response to salt and Cu^{2+} is consistent with earlier observations in *C. reinhardtii* [56], and *Euglena gracilis* [57], respectively.

Each of the acclimated strains displayed distinct metabolic fingerprints (Fig. 3 & 4). Furthermore, the FT-IR spectral analysis could distinguish between a stressed metabolic fingerprint and an acclimated metabolic fingerprint. Such a change to the metabolome due to acclimation has also been reported in response to high light acclimation in *C. reinhardtii*, where a metabolic fingerprint determined by nuclear magnetic resonance of acclimated high-light cells was distinct from both stressed, non-acclimated high-light cells and from non-stressed low-light cells [10]. There were contrasting features between the acclimation profiles particularly in terms of distinct carbon partitioning (Fig. 5). NH_4^+ treatment significantly increased amide peaks in comparison to non-stressed samples in acclimated and non-acclimated cells. This may indicate that increased protein synthesis is needed to deplete excess NH_4^+, which is a process known to occur in other microalgae [21]. Clearly additional metabolic features will explain these acclimation profiles and in future more targeted analysis will be able to identify specific metabolic pathways that are modified within these cells following the acclimation process.

A final experiment assessed how the acclimated cells tolerated a multiple stress environment, which can be considered as more analogous to a 'real' environment such as municipal wastewater. Again stressed and non-stressed cells were clearly distinguished, with the NH_4^+ acclimated cells largely indistinguishable from the non-acclimated stressed cells, the Cu^{2+} and PO_4^{3-} acclimated cells forming an adjacent cluster, and the Na^+ acclimated cells displaying a more distinct metabolic profile (Fig. 7). This correlates with the Na^+ acclimated cells being the only sample to show any enhanced tolerance to the multiple stressed condition. These cells had higher levels of amide peaks indicative of higher protein abundance, and which may suggest that these acclimated cells were more metabolically active under this multiple stress regime. This dependence on the Na^+ acclimated cells may also indicate that the tolerance to the Na^+ component of the multiple stress TAP medium is unique and could not be gained by the other acclimated cells, while the Na^+ acclimation

process partly allows tolerance of Cu^{2+}, PO_4^{3-} and NH_4^+ stress. This may in part be because the Na^+ exposure is the most toxic condition, thus the Na^+ acclimated cells may also show higher tolerance levels when exposed to the multiple stressed condition as it can withstand the most significant influencing factor. In addition, the process of acclimation may have led to physiological trade-offs that are less beneficial when the cells are exposed to a new environment [58].

This study has shown that acclimation to tolerate different ionic stresses by *C. reinhardtii* can be distinguished on the basis of metabolic signatures while some conserved features such as reduced accumulation of ROS and storage lipids were apparent. Future experiments will be needed to determine some of the specific mechanisms that underpin these acclimation processes. This may include a focus on the downstream signalling pathways that will result in acclimation. For example, acclimation to salinity in *C. reinhardtii* may be linked to Ca^{2+} signalling, lipid signalling and ROS signalling [9, 19, 59]. Finally, there will be interest to determine whether acclimation processes can be used to manipulate metabolism and biomass productivity of microalgae in order to enhance yields of particular metabolites that have high-value uses.

Acknowledgements

We thank Giles Johnson for assistance with chlorophyll fluorescence experiments and Olumayowa Osundeko for advice on oxidative stress experiments and comments to the manuscript.

Funding

This work was funded in part by a NATO Science for Peace and Security grant (Project No. G5320) to JKP. HM and RG thank the European Commission's Seventh Framework Program for funding (STREPSYNTH; Project No. 613877).

Author's contribution

EDC and JKP conceived and designed the project, EDC and HM performed experiments, and all authors were involved in analysis and interpretation of the data, and contributed to the manuscript writing.

References

[1] E. Nevo, Evolution under environmental stress at macro- and microscales, Genome Biol. Evol., 3 (2011) 1039-1052.

[2] M.A. Borowitzka, The 'stress' concept in microalgal biology—homeostasis, acclimation and adaptation, J. Appl. Phycol., in press (2018) doi: 10.1007/s10811-10018-11399-10810.

[3] Y. Tanaka, Y. Nishiyama, N. Murata, Acclimation of the photosynthetic machinery to high temperature in *Chlamydomonas reinhardtii* requires synthesis de novo of proteins encoded by the nuclear and chloroplast genomes, Plant Physiol., 124 (2000) 441-450.

[4] G. Bonente, S. Pippa, S. Castellano, R. Bassi, M. Ballottari, Acclimation of *Chlamydomonas reinhardtii* to different growth irradiances, J. Biol. Chem., 287 (2012) 5833-5847.

[5] M.-M. Perrineau, E. Zelzion, J. Gross, D.C. Price, J. Boyd, D. Bhattacharya, Evolution of salt tolerance in a laboratory reared population of *Chlamydomonas reinhardtii*, Environ. Microbiol., 16 (2014) 1755-1766.

[6] H.L. Johnson, J.L. Stauber, M.S. Adams, D.F. Jolley, Copper and zinc tolerance of two tropical microalgae after copper acclimation, Environ. Toxicol., 22 (2007) 234-244.

[7] C.-W. Chang, J.L. Moseley, D. Wykoff, A.R. Grossman, The *LPB1* gene is important for acclimation of *Chlamydomonas reinhardtii* to phosphorus and sulfur deprivation, Plant Physiol., 138 (2005) 319-329.

505 [8] J. Fan, l. Zheng, Acclimation to NaCl and light stress of heterotrophic *Chlamydomonas*
506 *reinhardtii* for lipid accumulation, J. Biosci. Bioeng., 124 (2017) 302-308.

507 [9] X. Chen, D. Tian, X. Kong, Q. Chen, A.A. E.F., X. Hu, A. Jia, The role of nitric oxide
508 signalling in response to salt stress in *Chlamydomonas reinhardtii*, Planta, 244 (2016) 651-
509 669.

510 [10] M.C. Davis, O. Fiehn, D.G. Durnford, Metabolic acclimation to excess light intensity in
511 *Chlamydomonas reinhardtii*, Plant Cell Environ., 36 (2013) 1391-1405.

512 [11] Y. Li, Y.-F. Chen, P. Chen, M. Min, W. Zhou, B. Martinez, J. Zhu, R. Ruan,
513 Characterization of a microalga *Chlorella* sp. well adapted to highly concentrated municipal
514 wastewater for nutrient removal and biodiesel production, Bioresour. Technol., 102 (2011)
515 5138-5144.

516 [12] O. Osundeko, H. Davies, J.K. Pittman, Oxidative stress-tolerant microalgae strains are
517 highly efficient for biofuel feedstock production on wastewater, Biomass Bioenergy, 56
518 (2013) 284-294.

519 [13] A.P. Dean, A. Hartley, O.A. McIntosh, A. Smith, H.K. Feord, N.H. Holmberg, T. King, E.
520 Yardley, K.N. White, J.K. Pittman, Metabolic adaptation of a *Chlamydomonas acidophila*
521 strain isolated from acid mine drainage ponds with low eukaryotic diversity, Sci. Total
522 Environ., 647 (2019) 75-87.

523 [14] J.K. Pittman, A.P. Dean, O. Osundeko, The potential of sustainable algal biofuel
524 production using wastewater resources, Bioresour. Technol., 102 (2011) 17-25.

525 [15] E.-S. Salama, M.B. Kurade, R.A.I. Abou-Shanab, M.M. El-Dalatony, I.-S. Yang, B. Min,
526 B.-H. Jeon, Recent progress in microalgal biomass production coupled with wastewater
527 treatment for biofuel generation, Renew. Sust. Energ. Rev., 79 (2017) 1189-1211.

528 [16] A. Ibuot, A.P. Dean, O.A. McIntosh, J.K. Pittman, Metal bioremediation by *CrMTP4*
529 over-expressing *Chlamydomonas reinhardtii* in comparison to natural wastewater-tolerant
530 microalgae strains, Algal Res., 24 (2017) 89-96.

531 [17] O. Osundeko, A.P. Dean, H. Davies, J.K. Pittman, Acclimation of microalgae to
532 wastewater environments involves increased oxidative stress tolerance activity, Plant Cell
533 Physiol., 55 (2014) 1848-1857.

534 [18] A.A.H. Khalid, Z. Yaakob, S.R.S. Abdullah, M.S. Takriff, Growth improvement and
535 metabolic profiling of native and commercial *Chlorella sorokiniana* strains acclimatized in
536 recycled agricultural wastewater, Bioresour. Technol., 247 (2018) 930-939.

537 [19] H.J.G. Meijer, J.A.J. van Himbergen, A. Musgrave, T. Munnik, Acclimation to salt
538 modifies the activation of several osmotic stress-activated lipid signalling pathways in
539 *Chlamydomonas*, Phytochemistry, 135 (2017) 64-72.

540 [20] A. Jamers, R. Blust, W. De Coen, J.L. Griffin, O.A.H. Jones, Copper toxicity in the
541 microalga *Chlamydomonas reinhardtii*: an integrated approach, BioMetals, 26 (2013) 731-
542 740.

543 [21] Y. Collos, P.J. Harrison, Acclimation and toxicity of high ammonium concentrations to
544 unicellular algae, Mar. Pollut. Bull., 80 (2014) 8-23.

545 [22] E.H. Harris, The Chlamydomonas Sourcebook, Academic Press, San Diego, 1989.

546 [23] H.K. Lichtenthaler, Chlorophylls and carotenoids: Pigments of photosynthetic
547 biomembranes, Methods Enzymol., 148 (1987) 350-382.

548 [24] K. Maxwell, G.N. Johnson, Chlorophyll fluorescence - a practical guide, J. Exp. Bot., 51
549 (2000) 659-668.

[25] H. Muhamadali, Y. Xu, D.I. Ellis, J.W. Allwood, N.J.W. Rattray, E. Correa, H. Alrabiah, J.R. Lloyd, R. Goodacre, Metabolic profiling of *Geobacter sulfurreducens* during industrial bioprocess scale-up, Appl. Environ. Microbiol., 81 (2015) 3288-3298.

[26] H. Martens, E. Stark, Extended multiplicative signal correction and spectral interference subtraction: new preprocessing methods for near infrared spectroscopy, J. Pharm. Biomed. Anal., 9 (1991) 625-635.

[27] H.J.H. Macfie, C.S. Gutteridge, J.R. Norris, Use of canonical variates analysis in differentiation of bacteria by pyrolysis gas-liquid chromatography, Microbiology, 104 (1978) 67-74.

[28] T. Driver, A.K. Bajhaiya, J.W. Allwood, R. Goodacre, J.K. Pittman, A.P. Dean, Metabolic responses of eukaryotic microalgae to environmental stress limit the ability of FT-IR spectroscopy for species identification, Algal Res., 11 (2015) 148-155.

[29] N. Mallick, F.H. Mohn, Reactive oxygen species: response of algal cells, J. Plant Physiol., 157 (2000) 183-193.

[30] L.M.L. Laurens, E.J. Wolfrum, Feasibility of spectroscopic characterization of algal lipids: Chemometric correlation of NIR and FTIR spectra with exogenous lipids in algal biomass, Bioenerg. Res., 4 (2011) 22-35.

[31] Y. Meng, C. Yao, S. Xue, H. Yang, Application of Fourier transform infrared (FT-IR) spectroscopy in determination of microalgal compositions, Bioresour. Technol., 151 (2014) 347-354.

[32] A.K. Bajhaiya, A.P. Dean, T. Driver, D.K. Trivedi, N.J.W. Rattray, J.W. Allwood, R. Goodacre, J.K. Pittman, High-throughput metabolic screening of microalgae genetic variation in response to nutrient limitation, Metabolomics, 12 (2016) 9.

573 [33] S.A. Patel, F. Currie, N. Thakker, R. Goodacre, Spatial metabolic fingerprinting using
574 FT-IR spectroscopy: investigating abiotic stresses on *Micrasterias hardyi*, Analyst, 133
575 (2008) 1707-1713.

576 [34] A.M.A. Pistorius, W.J. DeGrip, T.A. Egorova-Zachernyuk, Monitoring of biomass
577 composition from microbiological sources by means of FT-IR spectroscopy, Biotechnol.
578 Bioeng., 103 (2009) 123-129.

579 [35] S. Sithtisarn, K. Yokthongwattana, B. Mahong, S. Roytrakul, A. Paemanee, N.
580 Phaonakrop, C. Yokthongwattana, Comparative proteomic analysis of *Chlamydomonas*
581 *reinhardtii* control and a salinity-tolerant strain revealed a differential protein expression
582 pattern, Planta, 246 (2017) 843-856.

583 [36] G. Markou, K. Muylaert, Effect of light intensity on the degree of ammonia toxicity on
584 PSII activity of *Arthrospira platensis* and *Chlorella vulgaris*, Bioresour. Technol., 216 (2016)
585 453-461.

586 [37] H. Küpper, I. Šetlík, E. Šetliková, N. Ferimazova, M. Spiller, F.C. Küpper, Copper-
587 induced inhibition of photosynthesis: limiting steps of *in vivo* copper chlorophyll formation in
588 *Scenedesmus quadricauda*, Funct. Plant Biol., 30 (2003) 1187-1196.

589 [38] M. Bernal, M.V. Ramiro, R. Cases, R. Picorel, I. Yruela, Excess copper effect on growth,
590 chloroplast ultrastructure, oxygen-evolution activity and chlorophyll fluorescence in Glycine
591 max cell suspensions, Physiol. Plant., 127 (2006) 312-325.

592 [39] M. Kruskopf, K.J. Flynn, Chlorophyll content and fluorescence responses cannot be
593 used to gauge reliably phytoplankton biomass, nutrient status or growth rate, New Phytol.,
594 169 (2006) 525-536.

595 [40] I. Szivák, R. Behra, L. Sigg, Metal-induced reactive oxygen species production in
596 *Chlamydomonas reinhardtii* (chlorophyceae), J. Phycol., 45 (2009) 427-435.

[41] A. Podgórska, K. Gieczewska, K. Łukawska-Kuźma, A.G. Rasmusson, P. Gardeström, B. Szal, Long-term ammonium nutrition of *Arabidopsis* increases the extrachloroplastic NAD(P)H/NAD(P)+ ratio and mitochondrial reactive oxygen species level in leaves but does not impair photosynthetic capacity, Plant, Cell Environ., 36 (2013) 2034-2045.

[42] P.M. Glibert, F.P. Wilkerson, R.C. Dugdale, J.A. Raven, C.L. Dupont, P.R. Leavitt, A.E. Parker, J.M. Burkholder, T.M. Kana, Pluses and minuses of ammonium and nitrate uptake and assimilation by phytoplankton and implications for productivity and community composition, with emphasis on nitrogen-enriched conditions, Limnol. Oceanogr., 61 (2016) 165-197.

[43] A.A. Tammam, E.M. Fakhry, M. El-Sheekh, Effect of salt stress on antioxidant system and the metabolism of the reactive oxygen species in *Dunaliella salina* and *Dunaliella tertiolecta*, Afr. J. Biotechnol., 10 (2011) 3795-3808.

[44] S.E. Sabatini, Á.B. Juárez, M.R. Eppis, L. Bianchi, C.M. Luquet, M.d.C. Ríos de Molina, Oxidative stress and antioxidant defenses in two green microalgae exposed to copper, Ecotoxicol. Environ. Saf., 72 (2009) 1200-1206.

[45] S.M. Hamed, S. Selim, G. Klöck, H. AbdElgawad, Sensitivity of two green microalgae to copper stress: Growth, oxidative and antioxidants analyses, Ecotoxicol. Environ. Saf., 144 (2017) 19-25.

[46] D. Shukla, C.A. Rinehart, S.V. Sahi, Comprehensive study of excess phosphate response reveals ethylene mediated signaling that negatively regulates plant growth and development, Sci. Rep., 7 (2017) 3074.

[47] E. Kim, S. Yoo, H.-Y. Ro, H.-J. Han, Y.-W. Baek, I.-C. Eom, H.-M. Kim, P. Kim, K. Choi, Aquatic toxicity assessment of phosphate compounds, Environ Health Toxicol, 28 (2013) e2013002.

621 [48] M. Siderius, A. Musgrave, H. van den Ende, H. Koerten, P. Cambier, P. van der Meer,
622 *Chlamydomonas eugametos* (chlorophyta) stores phosphate in polyphosphate bodies
623 together with calcium, J. Phycol., 32 (1996) 402-409.

624 [49] Q. Li, L. Fu, Y. Wang, D. Zhou, B.E. Rittmann, Excessive phosphorus caused inhibition
625 and cell damage during heterotrophic growth of *Chlorella regularis*, Bioresour. Technol., 268
626 (2018) 266-270.

627 [50] M.J. Affenzeller, A. Darehshouri, A. Andosch, C. Lütz, U. Lütz-Meindl, Salt stress-
628 induced cell death in the unicellular green alga *Micrasterias denticulata*, J. Exp. Bot., 60
629 (2009) 939-954.

630 [51] J.K. Pittman, C. Edmond, P.A. Sunderland, C.M. Bray, A cation-regulated and proton
631 gradient-dependent cation transporter from *Chlamydomonas reinhardtii* has a role in calcium
632 and sodium homeostasis, J. Biol. Chem., 284 (2009) 525-533.

633 [52] Y. Jiang, Y. Zhu, Z. Hu, A. Lei, J. Wang, Towards elucidation of the toxic mechanism of
634 copper on the model green alga *Chlamydomonas reinhardtii*, Ecotoxicology, 25 (2016) 1417-
635 1425.

636 [53] M.S. Adams, C.T. Dillon, S. Vogt, B. Lai, J. Stauber, D.F. Jolley, Copper uptake,
637 intracellular localization, and speciation in marine microalgae measured by synchrotron
638 radiation X-ray fluorescence and absorption microspectroscopy, Environ. Sci. Technol., 50
639 (2016) 8827-8839.

640 [54] K.K. Sharma, H. Schuhmann, P.M. Schenk, High lipid induction in microalgae for
641 biodiesel production, Energies, 5 (2012) 1532.

642 [55] Y. Li-Beisson, F. Beisson, W. Riekhof, Metabolism of acyl-lipids in *Chlamydomonas*
643 *reinhardtii*, Plant J., 82 (2015) 504-522.

644 [56] M. Siaut, S. Cuine, C. Cagnon, B. Fessler, M. Nguyen, P. Carrier, A. Beyly, F. Beisson,
645 C. Triantaphylides, Y.H. Li-Beisson, G. Peltier, Oil accumulation in the model green alga
646 *Chlamydomonas reinhardtii*: characterization, variability between common laboratory strains
647 and relationship with starch reserves, BMC Biotechnol., 11 (2011) 7.

648 [57] M. Einicker-Lamas, G. Antunes Mezian, T. Benevides Fernandes, F.L.S. Silva, F.
649 Guerra, K. Miranda, M. Attias, M.M. Oliveira, *Euglena gracilis* as a model for the study of
650 Cu^{2+} and Zn^{2+} toxicity and accumulation in eukaryotic cells, Environ. Pollut., 120 (2002) 779-
651 786.

652 [58] C.T. Kremer, S.B. Fey, A.A. Arellano, D.A. Vasseur, Gradual plasticity alters population
653 dynamics in variable environments: thermal acclimation in the green alga *Chlamydomonas*
654 *reinhartdii*, Proc. R. Soc. B, 285 (2018) 20171942.

655 [59] P. Bickerton, S. Sello, C. Brownlee, J.K. Pittman, G.L. Wheeler, Spatial and temporal
656 specificity of Ca^{2+} signalling in *Chlamydomonas reinhardtii* in response to osmotic stress,
657 New Phytol., 212 (2016) 920-933.

658

Figures

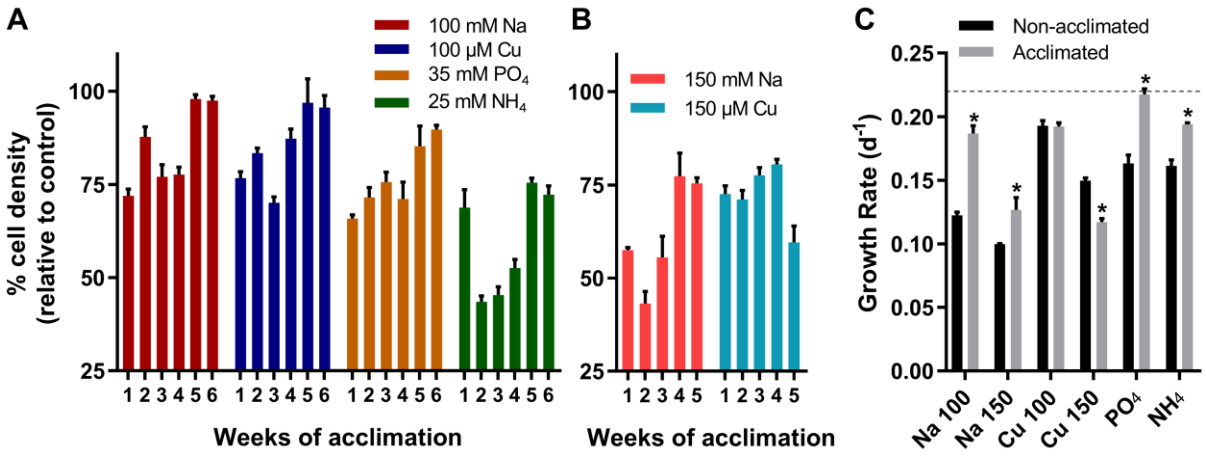

Fig. 1. Acclimating *Chlamydomonas reinhardtii* to excess Na^+, Cu^{2+}, PO_4^{3-} and NH_4^+. (A) Cell density after 7 d batch culture growth at each week of serial inoculation in TAP medium amended with 100 mM Na^+, 100 µM Cu^{2+}, 25 mM NH_4^+ and 35 mM PO_4^{3-}. (B) Cell density after 7 d batch culture growth at each week of serial inoculation of cells originally acclimated in 100 mM Na^+ and 100 µM Cu^{2+} grown in TAP medium amended with 150 mM Na^+ and 150 µM Cu^{2+}, respectively. Data shown (A and B) is cell density relative to non-stressed control cells. (C) Exponential phase growth rate for acclimated and non-acclimated cells grown in Na^+, Cu^{2+}, PO_4^{3-} or NH_4^+ conditions as indicated. All data are mean values ± SEM from 3 - 4 measurements. An asterisk (*) indicates significant difference ($p < 0.05$) of acclimated cells compared to non-acclimated cells. The dashed line indicates the mean non-stressed control value of growth rate.

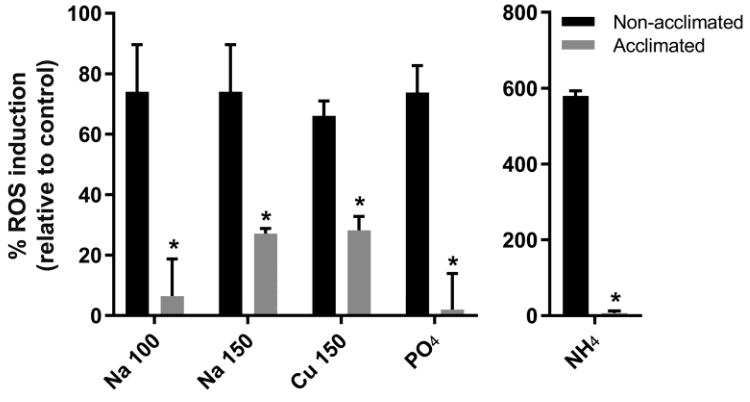

Fig. 2. Intracellular reactive oxygen species (ROS) induction in acclimated *Chlamydomonas reinhardtii* cells. ROS were determined by DCFH-DA staining after 3 h exposure to individual stresses in non-acclimated and acclimated cells. Data shown are ROS induction relative to non-stressed control cells. All data are mean values ± SEM from 3 measurements. An asterisk (*) indicates significant difference ($p < 0.05$) of acclimated cells compared to non-acclimated cells.

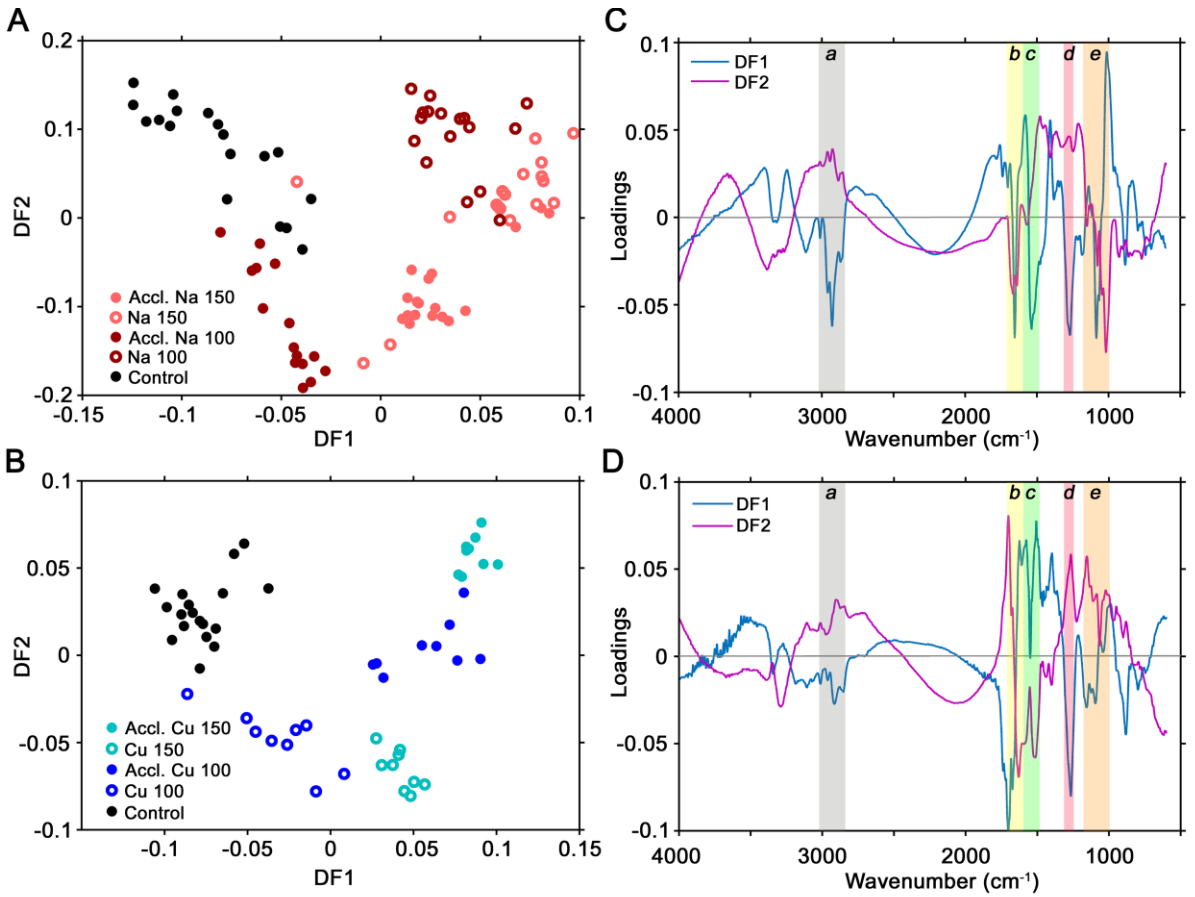

Fig. 3. FT-IR spectroscopy signatures in response to Na^+ and Cu^{2+} stresses in acclimated *Chlamydomonas reinhardtii* cells. (A and B) DF-PCA scores plot derived from replicate EMSC2 normalized spectra of acclimated (Accl.) and non-acclimated cells grown in Na^+ and Cu^{2+} conditions as indicated. Control cells were grown under non-stressed conditions. (C and D) DF1 and DF2 loading plots derived from the scores plots shown in panel (A) and (B). Key features of the spectra are highlighted: *a*, $\nu_s CH_2$ and $\nu_{as} CH_2$, $\nu_s CH_3$ and $\nu_{as} CH_3$ of fatty acids; *b*, νC=O of amides associated with protein (Amide I); *c*, δN-H of amides associated with protein (Amide II); *d*, ν_{as}P=O of nucleic acids, phosphoryl groups, phosphorylated proteins; *e*, νC-O of carbohydrates.

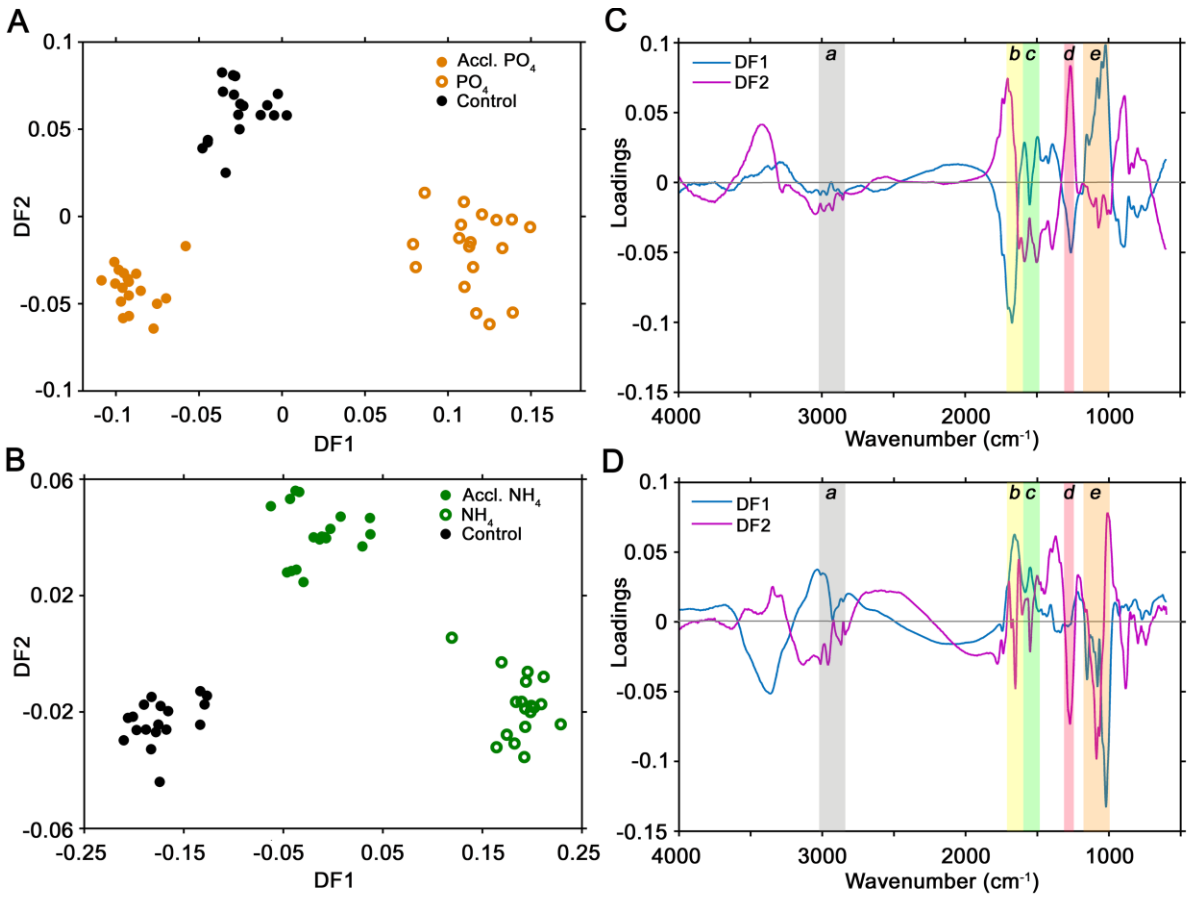

Fig. 4. FT-IR spectroscopy signatures in response to PO_4^{3-} and NH_4^+ stresses in acclimated *Chlamydomonas reinhardtii* cells. (A and B) DF-PCA scores plot derived from replicate EMSC2 normalized spectra of acclimated (Accl.) and non-acclimated cells grown in PO_4^{3-} and NH_4^+ conditions as indicated. Control cells were grown under non-stressed conditions. (C and D) DF1 and DF2 loading plots derived from the scores plots shown in panel (A) and (B). Key features of the spectra are highlighted: *a*, $\nu_s CH_2$ and $\nu_{as} CH_2$, $\nu_s CH_3$ and $\nu_{as} CH_3$ of fatty acids; *b*, νC=O of amides associated with protein (Amide I); *c*, δN-H of amides associated with protein (Amide II); *d*, ν_{as}P=O of nucleic acids, phosphoryl groups, phosphorylated proteins; *e*, νC-O of carbohydrates.

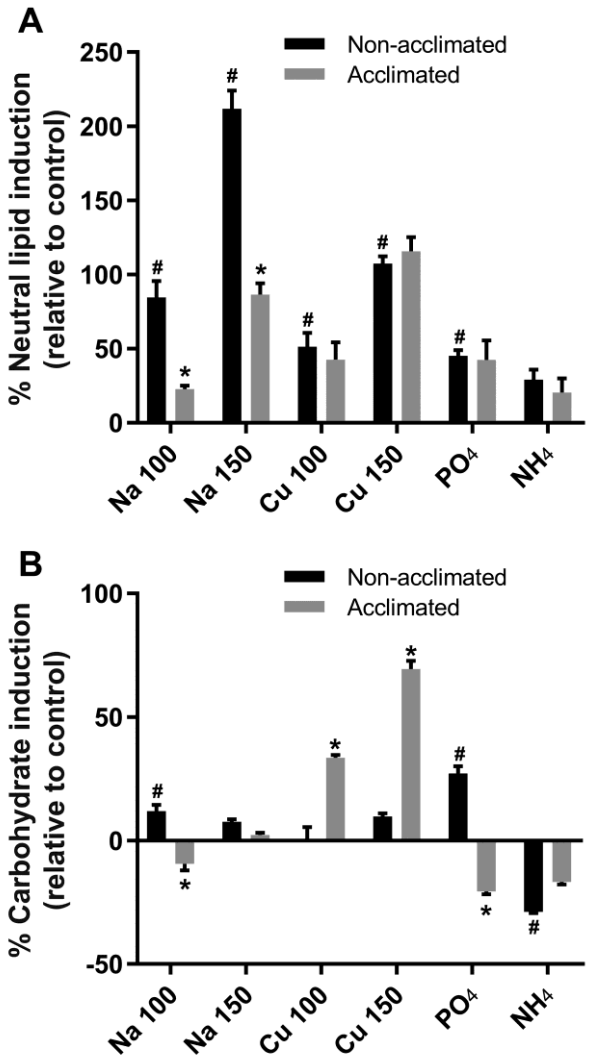

Fig. 5. Intracellular neutral lipid and carbohydrate induction in acclimated *Chlamydomonas reinhardtii* cells. (A) Neutral lipids were determined by Nile red staining after 6 d growth in individual stresses of non-acclimated and acclimated cells. (B) Carbohydrate values were determined by carbohydrate:amide I peak height ratio values from FT-IR spectra derived from cells after 6 d growth in individual stresses of non-acclimated and acclimated cells. Carbohydrate peaks were defined as those from wavenumber 1160, 1086, 1050 and 1036 cm^{-1} while the amide I peak was from 1655 cm^{-1}. Data shown are relative change in lipid or carbohydrate abundance relative to non-stressed control cells. All data are mean values ± SEM from 6 - 9 measurements. An asterisk (*), while a hash symbol (#) indicates significant difference ($p < 0.05$) of non-acclimated cells compared to control cells.

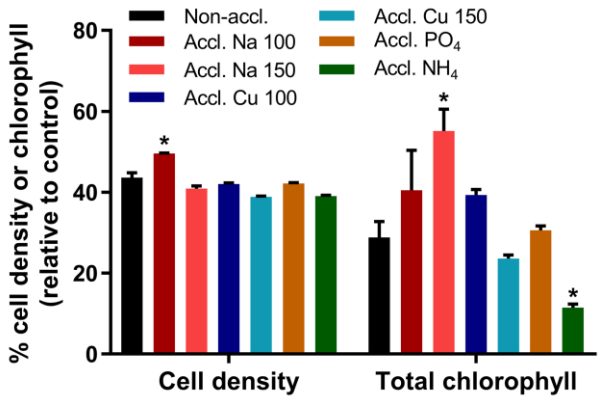

716

717 **Fig. 6**. Ability of single stress acclimated *Chlamydomonas reinhardtii* to tolerate multiple
718 stresses simultaneously. Cell density measured after 7 d growth and total chlorophyll
719 concentration measured after 4 d growth of acclimated and non-acclimated cells in a multi-
720 stress medium containing 100 mM Na^+, 100 µM Cu^{2+}, 25 mM NH_4^+ and 35 mM PO_4^{3-}.
721 Acclimated cells had been acclimated to each of the individual conditions as indicated. Data
722 shown are cell density or chlorophyll concentration relative to non-stressed control cells. All
723 data are mean values ± SEM from 3 measurements. An asterisk indicates significant
724 difference ($p < 0.05$) of acclimated cells compared to non-acclimated cells.
725

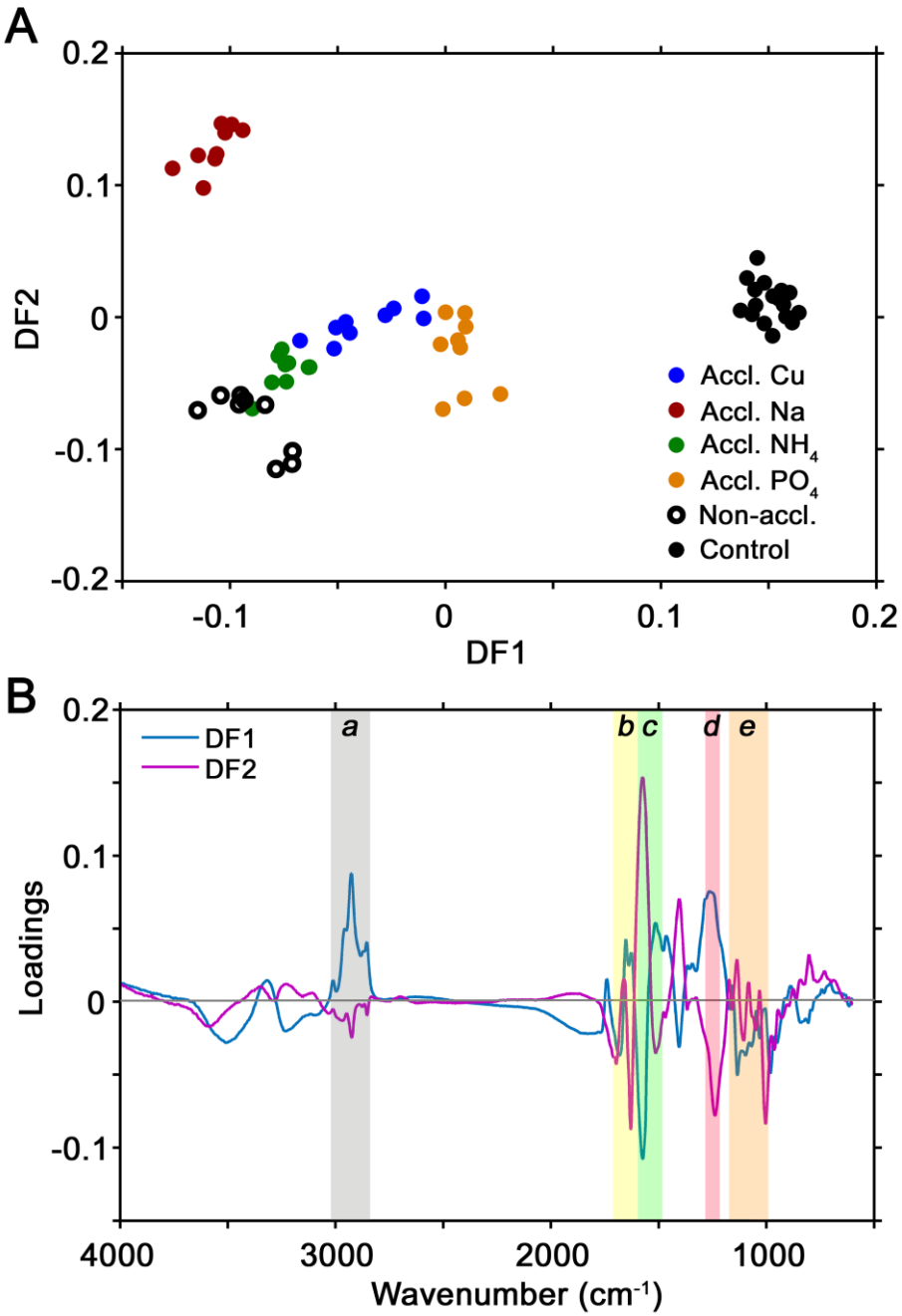

Fig. 7. FT-IR spectroscopy response to multiple stresses simultaneously in single stress-acclimated *Chlamydomonas reinhardtii* cells. (A) DF-PCA scores plot derived from replicate EMSC2 normalized spectra of acclimated and non-acclimated cells in a multi-stress medium containing 100 mM Na^+, 100 µM Cu^{2+}, 25 mM NH_4^+ and 35 mM PO_4^{3-}. Acclimated cells had been acclimated to each of the individual conditions as indicated. Control cells were grown under non-stressed conditions. (B) DF1 and DF2 loading plots derived from the scores plot shown in panel (A). Key features of the spectra are highlighted: *a*, $\nu_s CH_2$ and $\nu_{as} CH_2$, $\nu_s CH_3$ and $\nu_{as} CH_3$ of fatty acids; *b*, νC=O of amides associated with protein (Amide I); *c*, δN-H of amides associated with protein (Amide II); *d*, ν_{as}P=O of nucleic acids, phosphoryl groups, phosphorylated proteins; *e*, νC-O of carbohydrates.